ELSEVIER

Experimental Thermal and Fluid Science 18 (1998) 11–26

Experimental Thermal and Fluid Science

Particle dispersion in a turbulent round jet

Ian M. Kennedy *, Michael H. Moody

Department of Mechanical and Aeronautical Engineering, University of California, Davis, CA 95616, USA

Received 14 July 1997; received in revised form 29 January 1998; accepted 20 February 1998

Abstract

Particle dispersion and particle velocities were measured with laser sheets and a position sensitive photomultiplier tube to track particles. Monodisperse hexadecane droplets were injected onto the centerline of a turbulent air jet. Their radial dispersion, axial velocities, and times of flight were measured as functions of axial position. The time and length scales of the jet were varied through the control of the jet exit velocity and nozzle diameter. Nozzle diameters of 7 and 12.6 mm were used. Reynolds numbers were in the range of 10,000–32,400. Two different droplet diameters were used viz., 60 and 90 μm. A significant range in the Kolmogorov, turbulent, and acceleration Stokes numbers was covered. The times-of-flight were used to analyze the dispersion measurements in terms of Lagrangian statistics. Dispersion data at long times of flight for a range of nozzle diameters, particle diameters and exit velocities were analyzed to obtain the Lagrangian particle diffusivity. The non-dimensional diffusivities or Peclet numbers were found to approach a value that was similar to the Eulerian Peclet number for scalar transport in a jet. Furthermore, the particle dispersion increased linearly with time at long times from their release in the jet.

Keywords: Dispersion; Turbulence; Shear flow; Jet; Particles

1. Introduction

Many two phase flow systems rely on particle–turbulence interaction for mixing and dispersion. Examples include spray combustion systems, spray coating and painting, and pulverized coal furnaces. These systems may operate over a wide range of characteristic length and time scales for both the particle motion and the flow field. The description of such multiphase flows poses fundamental theoretical problems as well as difficulties in practical engineering modeling.

The simplest description of turbulent diffusion was proposed by Taylor [1] who developed the theory of 'diffusion by continuous movements' for the dispersion of a fluid particle. This fundamental theory described the statistical dispersion of fluid points in a stationary, homogeneous, turbulent flow. He derived the following well-known equation for the dispersion of a fluid particle in terms of a Lagrangian particle autocorrelation

$$\sigma(t)^2 = 2\int_0^t \int_0^{t'} \overline{v(t)^2}^{1/2}\,\overline{v(t')^2}^{1/2} R^{\mathrm{L}}(t,t')\,\mathrm{d}t'\,\mathrm{d}t, \tag{1}$$

where the dispersion $\sigma^2(t)$ is defined as the mean-square displacement from the origin, and the velocity autocorrelation coefficient R^{L} is defined by

$$R^{\mathrm{L}}(t,t') = \frac{\overline{v(t)v(t')}}{\left(\overline{v(t)^2}^{1/2}\,\overline{v(t')^2}^{1/2}\right)}, \tag{2}$$

where $t' = t + \theta$, with θ being the lag or separation time of the correlation. Two special cases of Taylors's theory are of interest here. For short times of flight: $\theta \to 0$ and it follows that $R^{\mathrm{L}}(0,t') \approx 1$ and $v(t) \approx v(0)$. Thus, the dispersion becomes quadratic with time i.e.,

$$\sigma^2 \approx \overline{v(0)^2} t^2. \tag{3}$$

For long times of flight, the integral of the autocorrelation function approaches a limiting value. Hence, it follows that the dispersion $\sigma^2(t)$ is a linear function of time and the diffusivity, defined as $\varepsilon \equiv \frac{1}{2}(\mathrm{d}\sigma^2/\mathrm{d}t)$, is a constant.

The theoretical description of particle dispersion in homogeneous turbulence has been extended by many investigators. Wang and Stock [2] developed an analysis of particles in homogeneous turbulence that included the crossing trajectories effect. They showed that if the gravitational drift velocity were unimportant, the long time diffusivity of a discrete particle could be larger than

* Corresponding author. Tel.: 1 530 752 2796; fax: 1 530 752 4158; e-mail: imkennedy@ucdavis.edu.

0894-1777/98/$19.00
PII: S0894-1777(98)10009-2

the fluid diffusivity. Dispersion in homogeneous turbulence has also been attacked by means of direct simulations of turbulence [3–7].

Free turbulent shear flows present difficulties in the analysis of dispersion because of the development of the flow field with position. Batchelor [8] showed that Taylor's theory for fluid particles could be extended to non-homogeneous, self-preserving flows, such as a round jet or a wake. He relied on the fundamental, heuristic assumption that the Lagrangian statistics of the flow were self-similar, in the same manner as the Eulerian statistics. The assumption is intuitively reasonable but it cannot be justified rigorously. Batchelor [8] was able to demonstrate that the asymptotic, long time dispersion of a fluid particle could be obtained through a relatively straightforward, one-dimensional analysis. Monin and Yaglom [9] derived similar but more general expressions for the dispersion tensor of fluid particles as a function of time. From these results, it was possible to show that the dispersion of a fluid particle should be a linear function of time in the case of a round, turbulent jet. Different scalings with time were possible for other types of shear flows. Experimental verification of the theory is not evident in the literature although many experimental investigations have been undertaken in relation to the dispersion of discrete (finite mass) particles.

Lagrangian measurements of particle motion and dispersion are most useful for comparisons with theory or computation. Unfortunately, they tend to be difficult experiments to perform. Snyder and Lumley [10] measured particle velocity autocorrelations in grid-generated turbulence with a photographic method. They showed that the autocorrelation of particle velocities decreased faster for heavier particles than lighter particles. All of the particles used in their experiment, except the hollow glass beads, had significant inertia effects.

Sato and Yamamoto [11] undertook a similar study of particle dispersion in grid turbulence with a more sophisticated optical arrangement. A light, responsive particle was used in this case to approximate a fluid particle. They measured the particle dispersion and the Lagrangian autocorrelation function as well as the Lagrangian integral length scale. The Lagrangian length scale was found to be smaller than the Eulerian length scale with a ratio that depended on the Reynolds number. Govan et al. [12] also used a photographic method to measure the radial dispersion of particles in a flow of gas through a pipe. The particles were relatively heavy and unresponsive to the turbulence. Lagrangian measurements of the particle motion were obtained. Nicolai et al. [13] used a more advanced solid state camera system to track particles in a suspension. They measured Lagrangian velocity autocorrelation functions and particle dispersion.

Many Eulerian studies have been concerned with the impact of particles on the gas phase turbulence [14]. There has also been considerable interest in the past decade with the details of the interaction between particles and flow structures. For example, Kobayashi et al. [15] found that particles were concentrated in the braid regions of a mixing layer, rather than in vortex cores. Kamalu et al. [16,17] also examined mixing layers with particles and reached almost the same conclusions as Kobayashi et al. [15]. They found that when the particle and flow time scales matched, the particles were dispersed more strongly than were smaller, nominally more responsive particles. Lázaro and Lasheras [18] demonstrated similar behavior by adding a polydisperse spray to a mixing layer that was forced periodically.

The examination of the detailed interaction of particles with well organized structures yields a valuable insight into particle dynamics. Although particles may exhibit anomalous dispersion when the particle response time and vortex time scale are of the same order, the amount of total dispersion downstream in a free shear flow is the integrated effect of many interactions, with continuously evolving fluid time scales. In practical terms, therefore, Lagrangian measurements of integrated or time averaged properties such as dispersion are valuable in testing and developing numerical models. Although the literature provides sets of data for particle dispersion and spreading in round jets, the measurements were purely Eulerian in nature and the addition of small amounts of solid or liquid phase material (as little as 2×10^{-6} volume fraction) was found to cause modification of the underlying carrier phase turbulence [19]. The modification of the carrier phase turbulence by the particles complicates the interpretation of experiments and modeling considerably because the impact is not well understood, even at the low loadings reported by Hetsroni and Sokolov [19].

Very few Lagrangian studies of the motion of fluid particles or heavy particles have been undertaken in free shear flows such as jets, mixing layers and wakes. Romano [20] measured the Lagrangian velocity autocorrelation function of flow following particles in a low Reynolds number water jet by particle tracking velocimetry. The pollen particles were believed to follow most of the motions of the turbulence. The cross stream dispersion of particles exhibited a quadratic dependence on time at short times and a linear behavior at long times, in agreement with the analysis of Batchelor [8]. Call and Kennedy [21,22] measured the dispersion of heavy particles in a round jet. They developed a particle tracking method to make particle dispersion measurements in a turbulent, round jet. A position sensing photomultiplier tube was used to measure the location of a single droplet as it passed through a laser sheet. The dispersion of the droplet was measured for a relatively narrow range of time and length scales of the jet and the droplet. A wider range of conditions is desirable so that models of particle dispersion can be tested over a range of ratios of characteristic particle response times to integral and Kolomogorov time scales of the carrier phase. The ratio of particle size to scales of the turbulence may be important through potential changes to the drag on particles. A fundamental outstanding question that can also be considered with these experiments is the relationship of Lagrangian to Eulerian statistics in a turbulent shear flow.

The experiments reported in this paper provide this set of Lagrangian data for an extremely dilute, two phase jet with absolute confidence that the gas phase turbulence is undisturbed by the addition of particles. The ultra dilute nature of the flow offers a considerable advantage to modelers in testing particle dispersion codes because the impact of the dispersed phase on the gas phase turbulence does not need to be considered.

2. Experimental techniques

A jet of room temperature air issued from a round nozzle into still air. The nozzle was designed to yield a "top hat" or uniform exit velocity. The jet was directed vertically downward. The experiment used hexadecane droplets that were more than 1000 droplet diameters apart. Consequently, there were no particle interactions and no modification of the gas phase turbulence. The particles were effectively non-vaporizing because the air was at room temperature (23°C) and the particles were measured in the flow for a relatively short time ($\ll$1 s). Monodisperse droplets were produced by a piezo-electric crystal. The crystal was a hollow cylinder with a liquid inlet on one side and a nozzle on the other. A pulse generator supplied a pulse of variable voltage, frequency and width to the crystal. This voltage caused the crystal to contract and push a small amount of liquid through the nozzle. Other details can be found in [21].

After the droplet was created, it was allowed to fall freely in the droplet shroud (Fig. 1). The shroud ensured that the droplet remained on the centerline of the flow. The air was straightened through screens and a honeycomb before it came into contact with the droplet. The air and droplet were then accelerated through the converging nozzle and the droplet entered the jet on the centerline. The variation in the velocities of droplets at the nozzle exit was less than 1% with this scheme of injection. Care was taken to shield the jet from disturbances in the laboratory with a mesh screen.

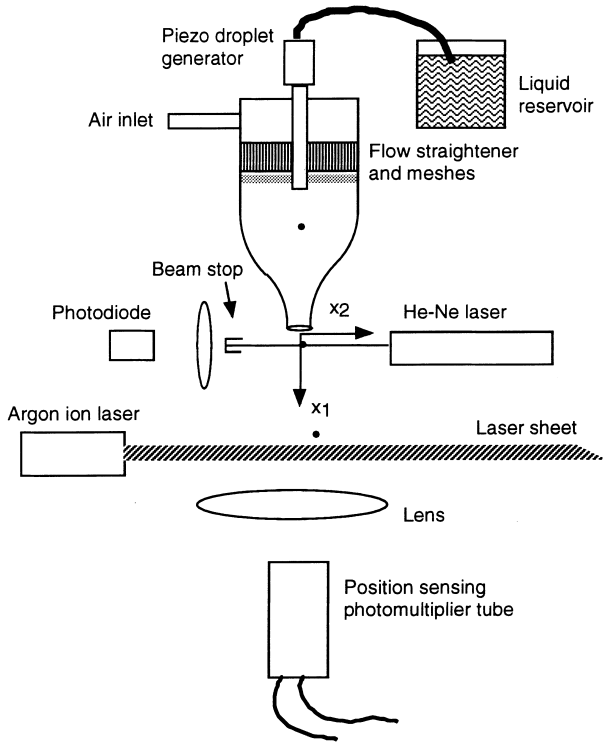

Fig. 1. Experimental setup.

The droplet detection system used a He–Ne laser that crossed the centerline of the nozzle exit. As a droplet left the nozzle, it crossed the laser beam, scattering light (Fig. 1) that was focused onto a photo diode. This voltage signal was used to trigger the data collection system.

Measurements of droplet position made use of a laser sheet that was formed by an argon-ion laser with associated optics (Fig. 1). As the droplet passed through the sheet, a collection lens formed an image of the droplet on the cathode of a position sensitive photomultiplier tube. The lens was located about 300 mm from the edge of the jet. Measurements of the velocity field (reported later) did not indicate any interference with the jet. The photomultiplier tube had four anode outputs whose magnitudes were proportional to the proximity of the centroid of the scattering image to the corresponding side of the detector. The signals were amplified before being digitized. At least 1000 droplets were measured in each case in order to give statistically meaningful results. The position of a particle was determined from scattering from one laser sheet. The time-of-flight of a particle from the instant it crossed the trigger beam at the nozzle exit was measured with an accuracy of ±2 ms. The position measurements were limited by the accuracy with which the photomultiplier detector could be calibrated with droplets of the same size as used in the experiment. The accuracy with which the location of a particle could be measured was ultimately determined by the scattered signal to noise level and, more importantly, by the quality of the image of the droplet on the photocathode. Hence, the resolution of position measurements was ±300 μm based on the repeatability of calibration measurements. Consequently, the relative systematic uncertainty in the reported values of dispersion was greatest for small dispersions, around ±12% for a dispersion of 25 mm^2, down to ±2% for a dispersion of 600 mm^2. Uncertainties in derived quantities were based on the square root of the sums of the squares of products of uncertainties in primary quantities with the corresponding partial derivative. Most of the measured values of dispersion were much greater than 25 μm so that typical uncertainties due to calibration errors were less than 5%. Furthermore, because the reported values of the dispersion are, in fact, a mean value that is an approximation to a true expectation of a distribution, there is an uncertainty due to sample size. The values of the dispersion that are reported overestimate the true mean-square displacement by approximately +6%.

Measurement of the axial component of the particle velocity, u, required the use of two laser sheets. The

sheets were created by directing the original laser sheet into a retro reflector that formed a second parallel laser sheet across the jet. The distance between the centers of the sheets was measured to give the length ΔL_u. The time between the peaks of scattering signals was calculated as follows. A Gaussian curve fit was applied to each signal with a linear regression performed on 31 data points. This process calculated the time of flight, Δt_u, between the sheets to $\pm\frac{1}{4}$ one clock pulse. Hence, the axial velocity, u, could be found from

$$u(x_1) = \frac{\Delta L_u}{\Delta t_u} \tag{4}$$

to within ±1%. In principle, the system should be capable of measuring the radial component of the droplet velocity. This component of velocity is more relevant to the radial dispersion than the axial velocity. However, it was found in practice that it was difficult to resolve accurately the rather small velocities in this direction with the present apparatus.

A TSI model 1053B hot wire anemometer was used for the velocity measurements of the air jet. The exit profiles for both the 7 and 12.6 mm nozzles are shown in Fig. 2. The figure shows a uniform or "top hat" exit velocity from both nozzles. The radial distance x_2 is normalized by the nozzle diameter D; the velocity u, is normalized by the centerline exit velocity U_c. The centerline exit velocities are given in Table 1.

Table 1
Centerline jet exit velocities

	Re_j		
	10 000	20 000	30 000
$D = 7$ mm			
U_c (m s^{-1})	21.5	43.0	64.5
$D = 12.6$ mm			
U_c (m s^{-1})	11.9	23.9	35.8

The axial mean velocities and turbulence intensities within the air jet were also measured. The centerline mean velocities and the intensities relative to the centerline mean velocity are shown in Fig. 3 for a nozzle diameter of 7 mm. The decay of mean velocity and the asymptotic level of turbulence intensity were typical of free turbulent jets. The results in the larger nozzle were similar. Measurements of the radial mean velocity profiles of the air at different axial positions (not shown) indicated that they were self-similar and that the jet maintained its axisymmetry.

3. Results

The behavior of a droplet in a turbulent jet is controlled by the local time and length scales of the flow

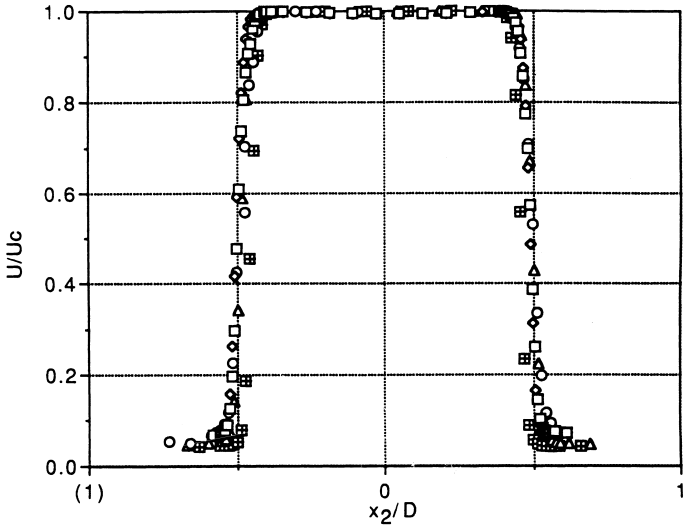

Figure 2. Profiles of the axial component of velocity at the nozzle exit normalized by the centerline velocity.

- Re = 20000, D = 12.6 mm
- Re = 30000, D = 12.6 mm
- Re = 10000, D = 7 mm
- Re = 20000, D = 7 mm
- Re = 30000, D = 7 mm

Fig. 2. Profiles of the axial component of velocity (U) at the nozzle exit normalized by the centerline velocity (U_C) for a range of Reynolds numbers (Re) and nozzle diameters (D).

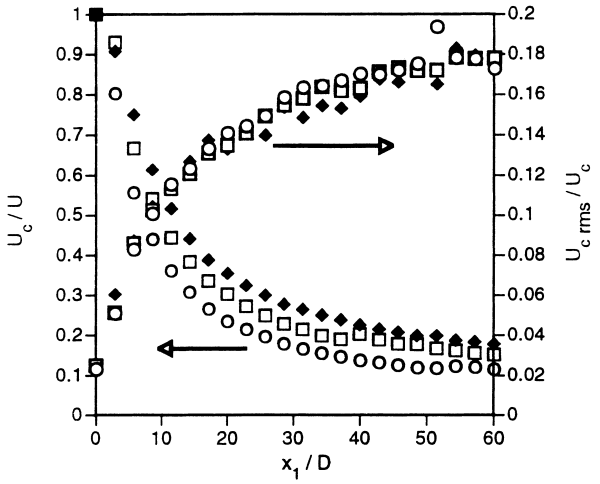

Fig. 3. Measurements of the mean axial velocity along the jet centerline (U) normalized by the centerline exit velocity (U_C); measurements of the relative turbulence intensity along the jet centerline ($U_{C\ rms}/U_C$). (♦) Reynolds number 10 000, (□) Reynolds number 20 000, (○) Reynolds number 30 000.

field and also by the characteristic time response of the droplet. The latter time scale is, of course, constant through the flow field. The time and length scales of the jet and of the droplet motion were varied by changing the nozzle exit velocity, the nozzle diameter and the droplet diameter.

3.1. Time scales

The droplet relaxation time can be estimated on the basis of Stokes flow as

$$\tau_d = \frac{\rho_d d_d^2}{18\mu}, \tag{5}$$

where ρ_d is the density of a droplet, d_d is the droplet diameter and μ is the gas viscosity. Values of τ_d are shown in Table 2. The particle response time can be non-dimensionalized by the convective time scale of the flow ($\tau_g = d/U$) to yield a characteristic nozzle Stokes number, $St = \tau_d/\tau_g$, also shown in Table 2.

Call and Kennedy [21] and Hardalupas et al. [14] used a time scale to characterize the slip due to deceleration in the mean gas velocity. This deceleration time scale is defined by

$$\tau_a = \left| \frac{d\overline{u}_g}{dx_1} \right|^{-1}, \tag{6}$$

where $\overline{u}_g$ is the mean velocity of the gas in the x_1 direction i.e., in the axial direction. The mean velocity measured by hot wire anemometry was differentiated to give the time scale, τ_a. This scale is smallest near the nozzle exit and increases monotonically as the jet develops. When $x_1/D > 40$, τ_a is considerably larger than the other scales and becomes unimportant. Inertial responses to the flow field can be described in terms of the acceleration Stokes number, S_m viz., the ratio of the particle response time, τ_d, to the fluid time scale for the change in the mean velocity. These ratios are shown in Table 2. A particle that is responsive to changes in the mean flow field has S_m less than unity everywhere; unresponsive particles exhibit an S_m greater than unity everywhere. Note that the present definition is consistent with our other usage of the Stokes number but it is the inverse of the definition of S_m used by Hardalupas et al. [14].

The time scale that characterizes the smallest eddies in a turbulent flow is the Kolmogorov time scale. The Kolmogorov time scale can be estimated from

$$\tau_k = \sqrt{\frac{\nu_g}{\varepsilon}}, \tag{7}$$

where ν_g is the gas kinematic viscosity and ε is the dissipation rate. Wells and Stock [23] used the ratio of particle response time τ_d and the Kolmogorov time scale τ_k to characterize the effects of particle inertia. If $\tau_d \approx \tau_k$ then the droplet can be expected to follow almost all gas fluctuations. The Kolmogorov Stokes numbers (τ_d/τ_k) for this experiment are shown in Table 2.

Shuen et al. [24] defined a turbulent Stokes number, S_T, that was the ratio of the droplet relaxation time to the time scale based on a characteristic eddy lifetime. This eddy lifetime was derived from

$$\tau_e = \frac{C}{\sqrt{\frac{2}{3}}} \frac{k}{\varepsilon}, \tag{8}$$

where k was the turbulent kinetic energy and C was a semi empirical coefficient set to 0.09. The turbulent kinetic energy and the dissipation rate were obtained from a Reynolds stress calculation of the jet [25]. This turbulent Stokes number is also shown in Table 2.

Wells and Stock [23] investigated the effect of body forces, such as gravity, on the so-called 'crossing trajectories' effect. They claimed that the impact of gravity was negligible when the drift or terminal velocity of the droplet, u_T, was less than the root mean square (r.m.s.) fluid velocity,

$$\sqrt{\overline{u}_g^2}.$$

The ratios of these velocities are given in Table 2 where it can be seen that the 'crossing trajectory' effect due to gravity should be unimportant. In general, the droplet Stokes numbers increase with increasing Reynolds number as the gas phase time scales become shorter. Conversely, the droplet Stokes numbers decrease with increasing distance from the nozzle as the length and time scales of the jet grow.

3.2. Length scales

A comparison of the droplet size with the size of the various length scales that characterize the turbulent flow field may be important. If the Kolmogorov scale is less than the diameter of the droplet, then the boundary layer around the particle may be modified and the drag may be changed. Antonia et al. [26] gave a relationship

Table 2
Time and length scales of hexadecane droplets in turbulent jets

Droplet diameter (μm)		60			90		
Jet nozzle diameter (*mm*): 7							
Re_j		10 000	20 000	30 000	10 000	20 000	30 000
τ_d (ms)			8.49			19.6	
Nozzle Stokes Number $\tau_d U/D$		26	53	77	61	122	178
Turbulent Stokes Number τ_d/τ_ε	$x_1/D = 25$	1.35	6.67	17.3	3.14	15.60	40.00
	$x_1/D = 40$	0.36	1.66	4.11	0.84	3.84	9.49
	$x_1/D = 50$	0.1 9	0.85	2.06	0.44	1.96	4.75
	$x_1/D = 60$	0.11	0.49	1.17	0.26	1.13	2.71
Kolmogorov Stokes Number τ_d/τ_k	$x_1/D = 25$	20.83	67.67	135.66	48.09	156.23	313.19
	$x_1/D = 40$	8.69	26.67	51.97	20.05	61.57	119.97
	$x_1/D = 50$	5.69	17.05	32.81	13.13	39.36	75.74
	$x_1/D = 60$	4.02	11.83	22.57	9.28	27.30	52.10
Acceleration Stokes number τ_d/τ_a	$x_1/D = 25$	0.27	0.46	0.57	0.63	1.1	1.3
	$x_1/D = 40$	0.13	0.24	0.26	0.31	0.55	0.60
Crossing trajectories ratio $u_T/\sqrt{u_g^2}$	$x_1/D = 25$	0.079	0.052	0.040	0.182	0.119	0.092
	$x_1/D = 40$	0.094	0.059	0.050	0.218	0.135	0.116
	$x_1/D = 50$	0.101	0.066	0.054	0.233	0.151	0.125
	$x_1/D = 60$	0.109	0.072	0.059	0.251	0.166	0.136
Kolmogorov length scale ratio d_d/η_k	$x_1/D = 25$	0.91	1.53	2.0736	1.36	2.29	3.10
	$x_1/D = 40$	0.57	0.95	1.29	0.85	1.43	1.94
	$x_1/D = 50$	0.45	0.76	1.03	0.68	1.15	1.55
Jet nozzle diameter (*mm*): 12.6							
Re_j		10 000	20 000	30 000	10 000	20 000	30 000
Response time τ_d (ms)			8.49			19.6	
Nozzle Stokes number $\tau_d U/D$		7.7	17	24	18	39	56
Turbulent Stokes number τ_d/τ_e	$x_1/D = 25$	0.23	1.16	2.93	0.53	2.67	6.77
	$x_1/D = 40$	0.06	0.29	0.70	0.14	0.66	1.61
	$x_1/D = 50$	0.03	0.14	0.35	0.07	0.33	0.80
	$x_1/D = 60$	0.02	0.08	0.20	0.04	0.19	0.46
Kolmogorov Stokes number τ_d/τ_k	$x_1/D = 25$	6.42	20.97	41.53	14.82	48.41	95.89
	$x_1/D = 40$	2.69	8.29	15.97	6.22	19.14	36.88
	$x_1/D = 50$	1.77	5.30	10.09	4.08	12.23	23.30
	$x_1/D = 60$	1.25	3.68	6.97	2.89	4.80	16.08
Acceleration Stokes number τ_d/τ_a	$x_1/D = 25$	0.12	0.14	0.25	0.28	0.31	0.57
	$x_1/D = 40$	0.034	0.095	0.11	0.079	0.22	0.26
Crossing trajectories ratio $u_T/\sqrt{u_g^2}$	$x_1/D = 25$	0.071	0.053	0.043	0.163	0.122	0.099
	$x_1/D = 40$	0.084	0.065	0.050	0.194	0.151	0.116
Kolmogorov length scale ratio d_d/η_k	$x_1/D = 25$	0.50	0.85	1.15	0.76	1.27	1.72
	$x_1/D = 40$	0.32	0.53	0.72	0.47	0.80	1.08
	$x_1/D = 50$	0.25	0.42	0.57	0.38	0.64	0.86
	$x_1/D = 60$	0.21	0.35	0.48	0.32	0.53	0.72

between the Kolmogorov Length scale η_k and the Reynolds number of the jet

$$\eta_k = (48\ Re_j^3)^{-1/4}(x_1). \quad (9)$$

The ratio of the droplet diameter and the Kolmogorov Length scale is shown in Table 2. As can be seen, this ratio is of order one. Hence, the potential exists for some impact on the drag of the particle.

3.3. Droplet dispersion

Particle dispersion, plotted in an Eulerian manner, is shown in Figs. 4 and 5 as a function of axial location x_1 normalized by the jet nozzle diameter D. Results over a range of jet Reynolds numbers Re_j are displayed in the figures. It can be seen that the smaller droplets responded more readily to the turbulence of the gas flow than the larger droplets and thus dispersed more. This was expected based on the time scale ratios given in Table 2. The smaller droplets have a shorter response time, allowing them to follow the flow to a greater extent than the larger particles.

The data shown in Figs. 4 and 5 can be replotted by using the average time-of-flight of the droplets to the measurement plane. The results for dispersion are presented in this "quasi-Lagrangian" form in Figs. 6 and 7. In fact, data that are plotted in this quasi-Lagrangian form are, in essence, the Eulerian data replotted with a transformed abscissa. However, because the time-of-flight and position were measured for each individual droplet, these data could be converted into true Lagrangian statistics. This was done by sorting the data

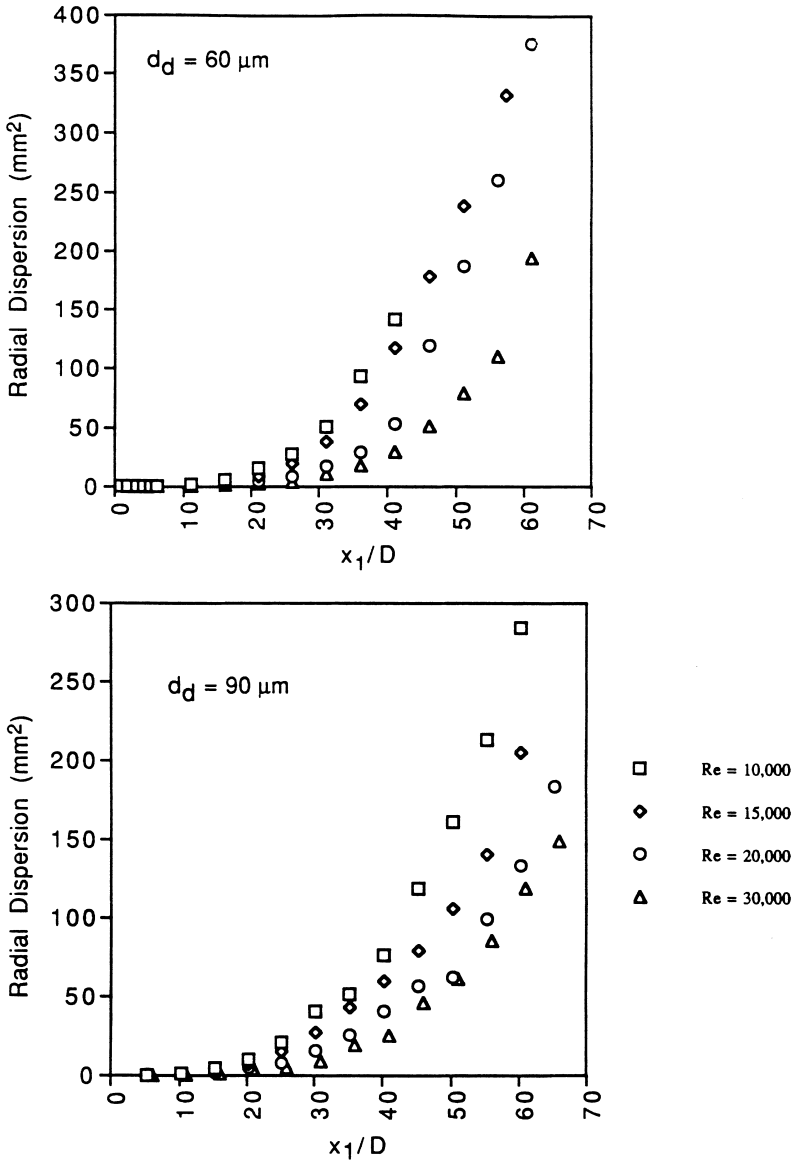

Fig. 4. Eulerian measurements of droplet dispersion with a 7 mm nozzle.

into small windows in time, on the order of the Kolmogorov time scale. The results of this manipulation of the data are shown in Fig. 8. It is apparent that the quasi-Lagrangian results approximate the true Lagrangian results very well for small times-of-flight and do not deviate significantly at larger times for a high Reynolds number. This is to be expected if the distribution of the times-of-flight is symmetrical about the mean as earlier studies showed [21] for a high Reynolds number jet. The agreement between the two sets of statistics is less satisfactory for the low Reynolds number situation as a result of the lack of development of the turbulence under these conditions.

In certain cases (when droplet velocity has equilibrated to the surrounding gas phase flow and the local Stokes number τ_a/τ_g reaches a small value within the domain of the measurements), the results for experimental dispersion exhibit two limiting cases. For short times-of-flight, the radial dispersion of a particle is quadratic in time and for long times-of-flight the dispersion is approximately linear in time. A similar behavior has been reported by Romano [20] for the dispersion of flow-following pollen particles in a turbulent jet of water. It is most clearly seen in experiments in which the Reynolds number is relatively low and, hence, in which the droplet exit velocity is relatively low. In the higher Reynolds number experiments, the droplets leave the nozzle with a higher velocity (see Fig. 8) and behave more like ballistic particles as the gas phase velocities drop rapidly downstream. In the linear regime, a particle diffusivity in the radial direction can be defined as $\frac{1}{2}(\mathrm{d}\sigma_d^2/\mathrm{d}t)$. The particle diffusivities were estimated for suitable cases in the near linear portion of the data towards the end of the droplet trajectory by using a least-squares fit. The

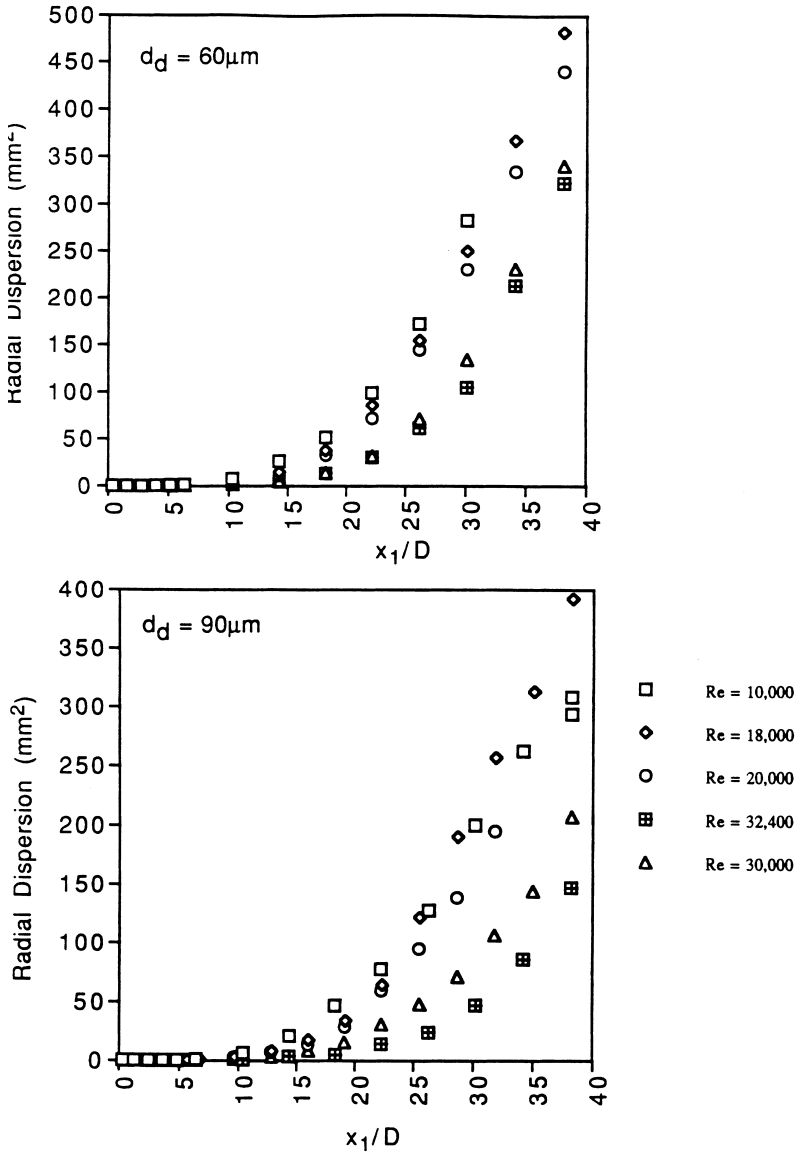

Fig. 5. Eulerian measurements of droplet dispersion with a 12.6 mm nozzle.

results, reported in Table 3, show an increasing trend with increasing Reynolds number.

For a given time-of-flight and a large exit velocity, a droplet will have traveled, on average, farther down stream than in a lower speed flow. In order to relate the data given in the Lagrangian form to the appropriate time scale, the turbulent time scales must be considered as functions of mean times of flight. The time scale ratios are given in Table 4 in this form for the range of experimental conditions.

As can be seen from the table, the larger droplets have the larger turbulent, Kolmogorov and acceleration Stokes numbers for a given jet Reynolds number. At a given mean time-of-flight, the turbulent Stokes number is smaller for the smaller Reynolds number flow. Hence, the droplets are more responsive to the turbulence at that time. It is also worth noting that the turbulent Stokes number varies by an order of magnitude over a time-of-flight from 5 to 25 ms as a result of the development of the jet. This observation illustrates the futility of assigning a single Stokes number to a particle in a rapidly developing flow such as the jet if the behavior of the particle in the far field is of interest.

3.4. Droplet velocities

The droplet axial velocities, $u_d(x_1)$, are shown in Eulerian form in Fig. 9 as a function of the axial distance from the 7 mm nozzle. It should be noted that the data were obtained across an entire section of the jet and are not conditioned upon the radial location i.e., the velocities are only functions of axial location, x_1. The mean velocities that were obtained in this manner were biased, therefore, by droplets that were close to

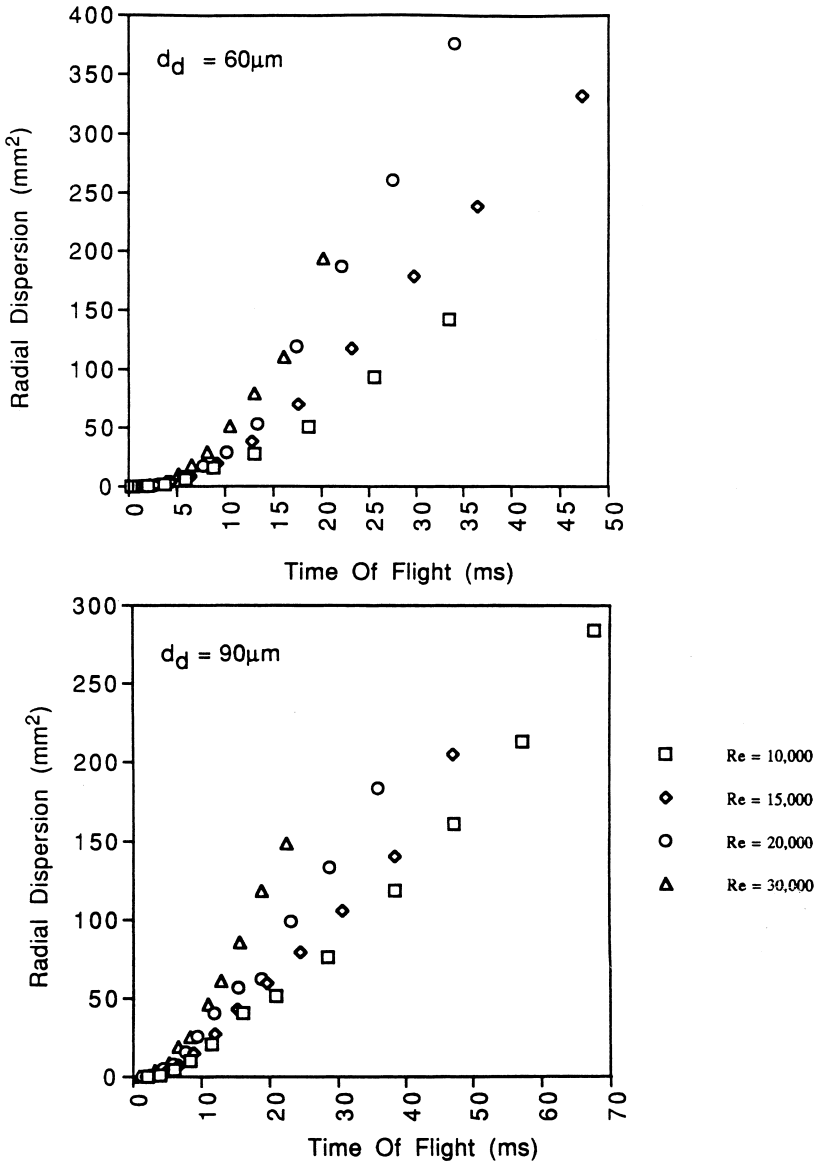

Fig. 6. Quasi-Lagrangian measurements of droplet dispersion with a 7 mm nozzle as function of mean time of flight from nozzle.

the axis because the greatest flux of droplets was found at this location. Hence, droplets near the axis of the jet provided the greatest contribution to the mean velocities that are reported in Fig. 8. Results from the 12.6 mm nozzle are very similar and hence are not shown here.

It can be seen from the velocity data at the nozzle exit that the droplets initially undergo some acceleration as they attempt to catch up to the air as it accelerates through the nozzle. A comparison of the droplet velocities with hot wire measurements of the air velocities (Table 1) indicates that there is a significant slip velocity between the phases near the nozzle exit with the droplets lagging the gas phase. As an example, the Reynolds number for flow around a 90 μm droplet at a nozzle Reynolds number of 30 000 approached values as high as 300 based on the relative velocity between the droplet and the gas. This is clearly well beyond the Stokes regime and calls into question the adequacy of τ_d, estimated using Stokes drag, as a measure of droplet response time.

4. Discussion

4.1. Scaling of droplet dispersion with time

Many factors in addition to simple drag forces can influence the dispersion of droplets in a turbulent flow. They include contributions from the virtual mass and Bassett history terms in the equation for particle motion [27] as well as lift forces [28]. Faeth [28] showed that the virtual mass and Bassett terms were not important for

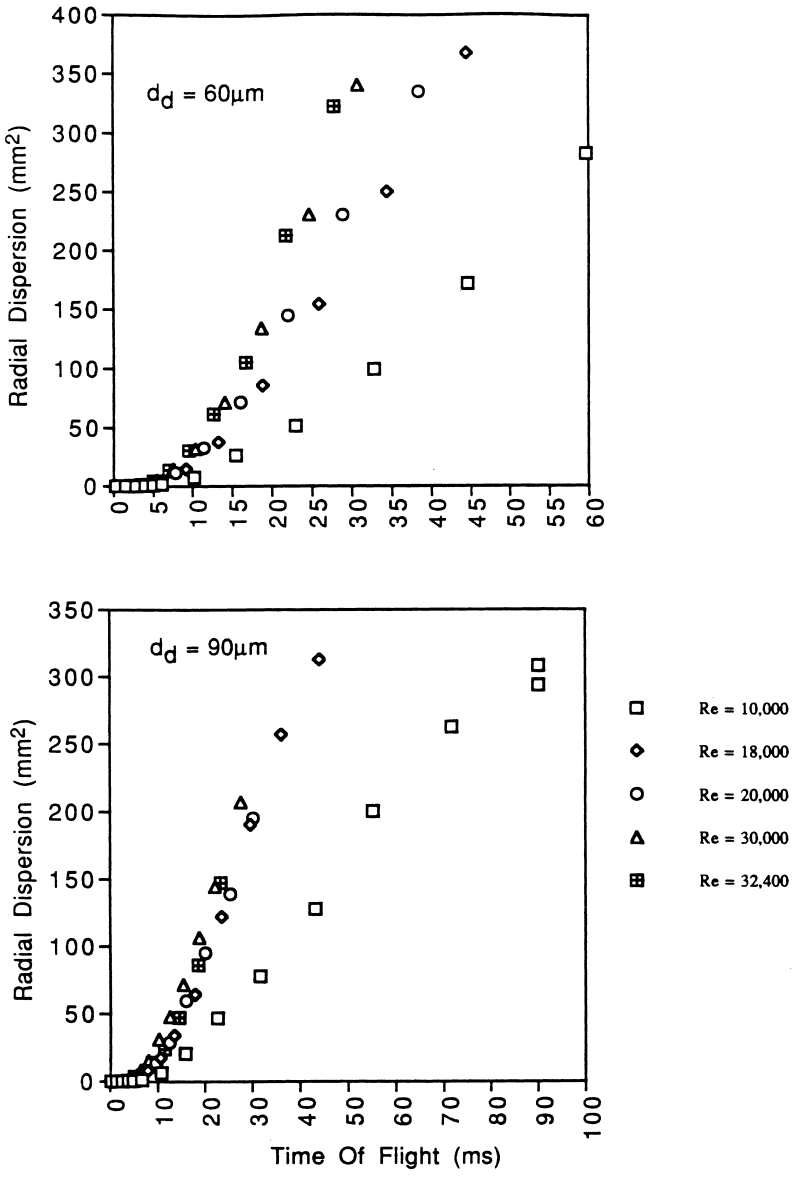

Fig. 7. Quasi-Lagrangian measurements of droplet dispersion with a 12.6 mm nozzle as function of mean time of flight from nozzle.

liquid droplets dispersed in air at a pressure of one atmosphere. Furthermore, he concluded that Saffman lift forces [29] were an order of magnitude less than the drag force for droplet diameters less than the nozzle diameter at axial locations of $x_1/D > 10$, conditions that pertain to the present investigation. Droplet rotation could conceivably be induced by the piezo-electric generation process. However, the droplet is directed down a long straight tube without difficulty. The droplets leave the nozzle completely aligned with the centerline of the jet. Hence, there is no evidence of lift induced by a Magnus effect. It is also possible that the droplets are distorted by the relative velocity difference between them and the gas phase. An estimate of the Weber number for the droplets in the worst case situation, where velocity differences are greatest, shows that it is much less than one, indicating the dominance of surface tension and the likelihood that the droplets remain spherical.

The dispersion of particles exhibits a quadratic behavior with time for short times-of-flight. The dispersion is approximately linear with time for long times-of-flight. This observation invites a comparison with Taylor's [1] results for the dispersion of a fluid particle in a homogeneous, stationary turbulence with the strong *caveat* that the motion of droplets in a jet are far from the conditions considered by Taylor. In this case, it is recalled that the dispersion was also a linear function of time. Batchelor [8] and Monin and Yaglom [9] argued heuristically that it was possible to scale the velocity of a *fluid* particle in a self-preserving flow, such as a jet, so that the velocity and other statistics became statisti-

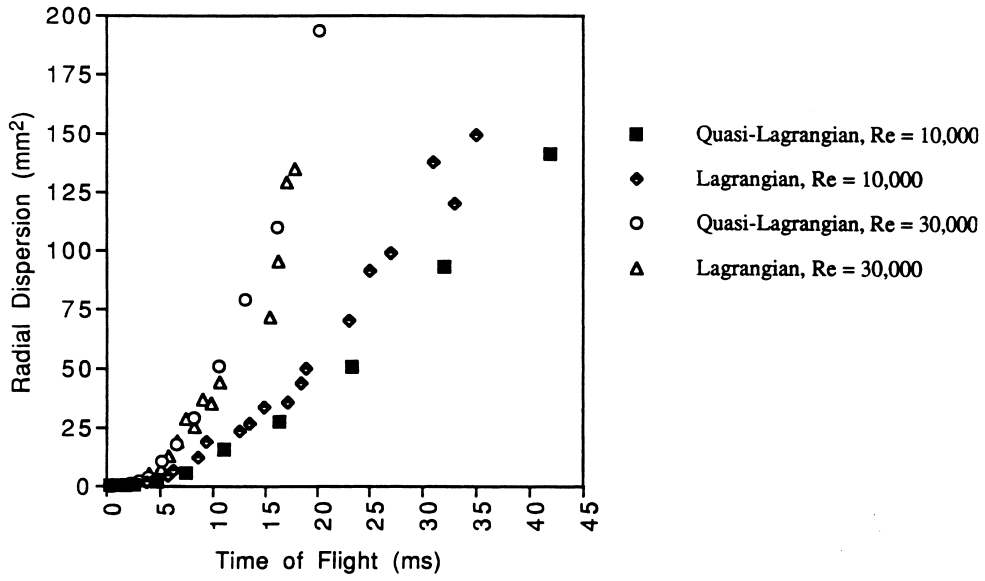

Fig. 8. Quasi-Lagrangian and Lagrangian measurements of particle dispersion with a 7 mm nozzle.

Table 3
Particle diffusivities

	Re_j		
	15 000	20 000	30 000
$D = 7$ mm			
ε_d (m^2s^{-1}) ($d_d = 60$ μm)	0.0042	0.0079	0.010
$D = 12.6$ mm			
ε_d (m^2s^{-1}) ($d_d = 60$ μm)	0.0053	0.0058	0.0076

cally stationary. The particle diffusivity in the radial direction for a round jet can be written as

$$\varepsilon = \frac{1}{2}\frac{d\sigma_d^2}{dt} = \frac{1}{2}\frac{d}{dt}\langle x_2(t)\, x_2(t)\rangle, \tag{10}$$

where x_2 is the particle displacement in the radial direction. Batchelor's [8] analysis can be used to show that the diffusivity of a *fluid* particle in a round jet is constant and the dispersion itself varies linearly with t. This result depends upon the scaling of the mean downstream location of the fluid particle with time-of-flight as $t^{1/2}$ and

Table 4
Stokes numbers as functions of time-of-flight

Droplet diameter (μm)		60			90		
$D = 7$ mm							
Re_j		10 000	20 000	30 000	10 000	20 000	30 000
Turbulent Stokes number τ_d/τ_e	$t = 5$ ms	5.92	6.55	9.05	14.4	15.9	19.2
	$t = 15$ ms	1.05	1.39	1.63	2.14	2.84	3.16
	$t = 25$ ms	0.50	0.68	0.75	1.04	1.38	1.44
Kolmogorov Stokes number τ_d/τ_k	$t = 5$ ms	54.8	66.2	88.2	131	158	192
	$t = 15$ ms	17.5	23.6	28.1	37.3	50.3	57.9
	$t = 25$ ms	10.7	14.7	16.8	23.1	31.1	34.4
Acceleration Stokes number τ_d/τ_a	$t = 5$ ms	0.18	0.42	0.35	1.4	1.3	0.69
	$t = 10$ ms	0.085	0.26	0.19	0.71	0.85	0.35
$D = 12.6$ mm							
Re_j		10 000	20 000	30 000	10 000	20 000	30 000
Turbulent Stokes number τ_d/τ_e	$t = 25$ ms	0.53	0.89	1.11	1.14	1.81	1.97
	$t = 30$ ms	0.39	0.67	0.83	0.85	1.32	1.44
	$t = 40$ ms	0.25	0.43	0.53	0.54	0.81	0.89
Kolmogorov Stokes number τ_d/τ_k	$t = 25$ ms	11.1	17.5	21.7	24.4	37.3	42.2
	$t = 30$ ms	9.13	14.5	17.9	20.1	30.3	34.4
	$t = 40$ ms	6.75	10.9	13.3	15.0	21.8	25.0
Acceleration Stokes number τ_d/τ_a	$t = 25$ ms	0.25	0.12	0.14	0.070	0.29	0.25
	$t = 30$ ms	0.19	0.11	0.12	0.062	0.27	0.21

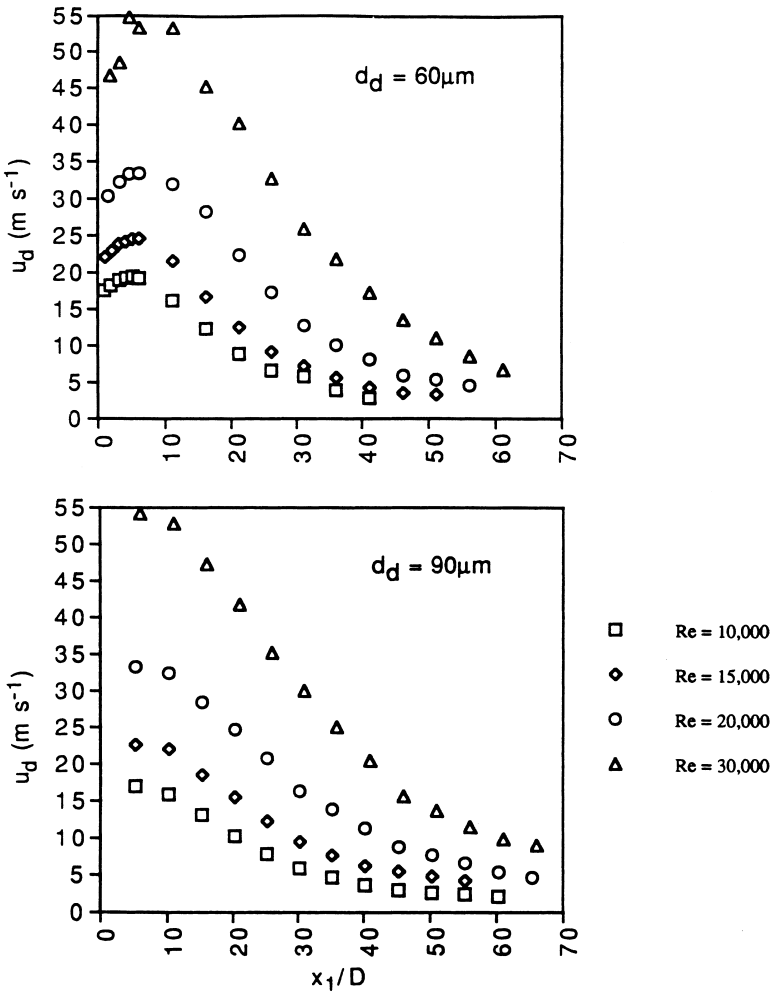

Fig. 9. Mean droplet velocities, u_d, as a function of downstream location with a 7 mm nozzle.

the velocity scale with $t^{-1/2}$, results that lead to a time scale for fluctuations in the *fluid* particle velocity that itself varies linearly with t. Monin and Yaglom [9] obtained a more general expression for the dispersion tensor but the arguments are essentially the same.

A discrete particle will not behave in the same manner as a fluid particle due to its finite size and mass. Its inertia will not permit it to respond to all the fluctuations of the surrounding fluid. However, one would expect that the particle would eventually respond to most of the significant fluid motions in a developing flow such as a jet when the local, particle Stokes number (based on the particle response time scale τ_d that is fixed and the fluid time scale τ_g that grows linearly with time in a jet as shown above) is less than one. This does not take into account the velocity difference between the droplet and the gas phase. If the velocity difference is large as a result of the droplet's inertia, then the interaction time between a droplet and an eddy will be less than τ_g. In these cases, the appropriate fluid time scale would be the transit time of a droplet across an eddy, found in the manner used in stochastic simulations of two phase flows [30]. The transit time is less than the eddy life time. Hence, significant slip between the phases would lead to a larger Stokes number as τ_g decreased. If this issue is ignored, the particle Stokes number, St, will decrease with time-of-flight as t^{-1}

$$\mathrm{St} = \frac{\tau_a}{\tau_g} \sim t^{-1}. \tag{11}$$

It can be shown that a *fluid* particle will disperse linearly with time-of-flight t by noting that the mean, downstream location of the particle scales $\bar{x}(t) \sim t^{1/2}$. One would expect that a *discrete* particle in a flow with a very small Stokes number would exhibit a similar behavior i.e., it would behave as flow tracer. It is not immediately apparent whether particles with Stokes numbers of O(1) or greater will deviate significantly from this scaling of downstream location with time in a jet. A simple analysis of the mean motion of a discrete particle can be used to examine the impact of Stokes number variations on the response of a particle to changes in the mean velocity field of the gas. Assuming a Stokes drag law and a suitable description of a mean ax-

ial velocity in a turbulent jet, the response of a particle to the mean fluid motion can be described approximately (by neglecting turbulent fluctuations) in terms of non-dimensionalized equations as

$$\frac{d^2\tilde{u}}{d\tilde{t}^2} = \frac{1}{St}\left(\frac{a}{\tilde{x}+b}\right), \tag{12}$$

$$\frac{d\tilde{x}}{d\tilde{t}} = \tilde{u}, \tag{13}$$

where the particle velocity u is non-dimensionalized by the particle velocity, U, at the nozzle exit

$$\tilde{u} = \frac{u}{U}, \tag{14}$$

the non-dimensional particle time-of-flight is

$$\tilde{t} = \frac{tU}{D} \tag{15}$$

and the non-dimensional axial location of the particle is

$$\tilde{x} = \frac{x}{D}. \tag{16}$$

The parameters a and b were chosen to provide a reasonable representation of the mean axial velocity in the jet. This non-linear set of equations is not amenable to a simple analytical solution. Matched asymptotics [31] can be used to show that for $St \ll 1$,

$$\tilde{x} \sim \tilde{t}^{1/2} \tag{17}$$

to first order.

A more general solution can be obtained with a fourth-order Runge Kutta method for a range of characteristic Stokes numbers. The results are shown in Fig. 10 for $St = 1.0$, 10 and 100. It appears that the mean downstream location scales quite closely with $t^{1/2}$ (i.e., the curves are linear on this plot) over a wide range of Stokes numbers. Results for $St = 0.1$ are indistinguishable from the results for $St = 1.0$ and 10. The behavior at large Stokes number is different at small non-dimensional distance from the nozzle but it fairly quickly assumes the same form as the other cases. Hence, one can expect that the fluid time scale to which the particle is exposed scales approximately with the time-of-flight, t, for Stokes numbers less than about 10. However, if the local Stokes number St (based on the local turbulence integral time scale or the large eddy lifetime, τ_g (Eq. (8))) is greater than 1 then the filtering of the turbulent motion by the particle inertia may be significant. Consequently, the particle time scale τ_d would be important and one would not expect the analysis of Batchelor [8] or Monin and Yaglom [9] to pertain. A more restrictive criterion would require the local Stokes number to be less than 1.

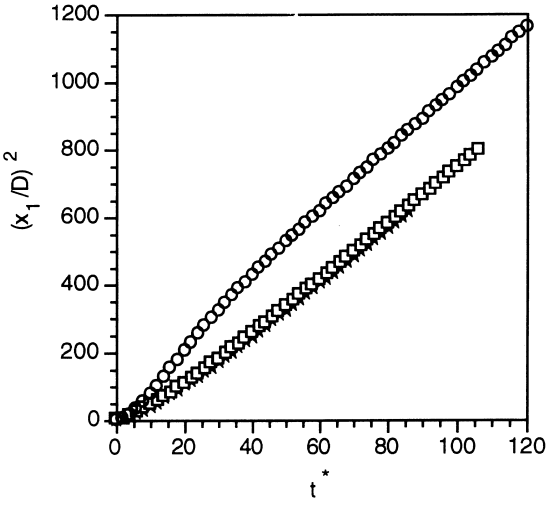

Fig. 10. Numerically calculated non-dimensional downstream distance squared as a function of a particle's non-dimensional time of flight $t^* = tU/D$ at various particle Stokes numbers $St = \tau_d U/D$. (★) $St = 1.0$, (□) $St = 10$, (○) $St = 100$.

The local fluid time scale was estimated from the results of a Reynolds stress model. The ensuing turbulent Stokes numbers at different times-of-flight from the nozzle are shown in Table 4. It is apparent that the 60 μm droplets attain a turbulent Stokes number of approximately one at a time of about 20 ms with both nozzles. This estimate appears to be reasonable in comparison to the apparent onset of the linear regime in Figs. 6 and 7. The dispersion at a Reynolds number of 10 000 does not become truly linear because the turbulence is not fully developed. At Reynolds numbers of 15 000 and greater, the dispersion becomes approximately linear with time after about 20 ms. The estimates in Table 4 suggest that the 90 μm droplets require times-of-flight in excess of 25 ms to achieve a Stokes number of unity.

4.2. Droplet diffusivities and Peclet numbers

The slope of the particle dispersion curves was measured over their straight sections i.e., after a "long" time-of-flight, to obtain an estimate of the Lagrangian particle diffusivity, ε_p^L. This diffusivity was non-dimensionalized with the convective time scale of the jet to yield a Lagrangian Peclet number

$$Pe_p^L = \frac{UD}{\varepsilon_p^L}. \tag{18}$$

Based on the measurements of van der Hegge Zijnen, Hinze [32] indicated that the Eulerian eddy viscosity of fluid in a round jet could be expressed in terms of the square root of the jet momentum flux as

$$\varepsilon_m^E = 0.0116\ UD. \tag{19}$$

This relationship was obtained by fitting a velocity profile to experimental data under the assumption of a constant eddy viscosity. The assumption of a constant eddy viscosity throughout the jet is not entirely correct. Furthermore, the concept of an eddy viscosity is intrinsically flawed in a shear flow but it suffices to yield an estimate of the characteristic rate of turbulent transport of momentum. Chevray and Tutu [33] made detailed measurements of the velocity and temperature fields in a slightly heated turbulent round jet. They reported values of the turbulent Prandtl number

Table 5
Particle numbers for 60 μm droplets

	Re_j	
	20 000	30 000
$D = 7$ mm	39	43
$D = 12.6$ mm	53	59

$$Pr_T = \frac{\varepsilon_m^E}{\varepsilon_T^E} \tag{20}$$

that varied across the jet from a value of about 0.4 to a maximum of about 0.7. If a typical value of $Pr_T = 0.6$ is used, then the eddy diffusivity, ε_T^E, is approximately (0.02 *UD*). This leads to an estimate of the Eulerian Peclet number of about 50.

The measured Lagrangian particle Peclet numbers are shown in Table 5 for those cases where dispersion was linear with time for a significant period i.e., for the 60 μm droplets in jets with Reynolds numbers greater than 20 000. Analysis showed that the uncertainty in the Peclet number was dominated by the uncertainty in the estimation of the diffusivity, ε_p^L. The uncertainty in the Peclet number for the worst case (largest velocity and diameter) was estimated to be ±8. The results are close to the estimated Peclet number for the transport of heat, given the error inherent in the differentiation of experimental data. The similarity in the values of the Lagrangian and the Eulerian diffusivities is rather surprising in view of the difference in definitions of the two quantities. It is possible, in fact, to equate directly the Lagrangian diffusivity (Eq. (10)) with the eddy diffusivity in the case of stationary, homogeneous turbulence when the probability density function for particle location is Gaussian [1]. The extension of this equality to a round, turbulent jet is rather problematical.

However, the probability density function for particle location has been found to be Gaussian by Call and Kennedy [21]. This observation, in conjunction with Batchelor's [8] demonstration that the self-preserving feature of the flow can be used to derive a scaling of the particle dispersion as a function of time, suggests a similar theoretical association between the eddy diffusivity and the Lagrangian diffusivity in the round jet. The present experimental results suggest a simple and direct relationship between the two quantities.

None of the results suggests the possibility of a particle diffusivity in the far field of the round jet that is significantly greater than the fluid diffusivity, in contrast to findings in two-dimensional shear layers [34]. It must be emphasized that the results apply only to times that are long compared to a characteristic Lagrangian length scale, or equivalently, to locations far from the source or nozzle. Over this period, droplets have been exposed to many eddies of widely varying time and length scales and a wide range of values of the turbulent Stokes numbers have been covered over a droplet trajectory. Hence, preferential dispersion of particles by vortices with time scales of the same magnitude as the droplet response time scale is not likely to be evident in the statistics of far field dispersion.

Other physical processes may influence particle dispersion. Gravity may play a role although the estimates that were shown in Table 2 suggest that the gravitational effect is generally not important. Another potentially important issue relates to the impact of flow unsteadiness on the drag around a droplet. Estimates of the Kolmogorov scales in the flow indicate that they can be comparable to the size of the droplets. A modification to the boundary layer around the droplet and its drag may result in some variation in the particle diffusivity. Any effects due to the variation of the length and time scales of the turbulence in relation to the size of the droplets were small over the limited range of conditions. Although a trend can be discerned in Table 5, it is within the estimated uncertainty and the ensuing discussion must be viewed in this light. As the nozzle diameter decreases, the Peclet number decreases at a fixed Reynolds number, suggesting that the particle diffusivity may not scale *solely* with the jet time scale and length scale. As the nozzle diameter decreases, the length scales of the jet decrease commensurately; the time scales decrease with nozzle diameter squared for a constant Reynolds number. Hence, a droplet will experience smaller scale turbulence and greater unsteadiness as the nozzle diameter is reduced. Odar and Hamilton [35] and Karanfilian and Kotas [36] showed for small and large Reynolds numbers, respectively, that the drag coefficient on a small sphere increased as a result of unsteadiness in the surrounding flow, depending on the magnitude of the disturbance via a so-called acceleration number. This increase in drag would be manifested in the present experiment as an apparent increase in the particle diffusivity, leading to a reduction in the particle Peclet number as the nozzle diameter decreased, as seen in Table 5. Unfortunately, the trend seen in Table 5 is not definitive; data over a wider range of nozzle sizes are required for confirmation.

5. Practical usefulness and significance

A complete set of data is provided for comparison with calculations of particle dispersion in a turbulent shear flow. In contrast to other reported data, the current results document thoroughly the initial conditions of the flow field. Furthermore, the addition of the particles to the jet does not affect the gas phase flow at all so that calculations of the particle dispersion can be decoupled from calculations of the flow field. The similarity of the measured Lagrangian particle diffusivity and the eddy diffusivity of the jet suggest the possibility of reducing

[1] Monin and Yaglom [9], Vol. 1, Section 10.3 demonstrated the equivalence of the two quantities by substituting the Gaussian distribution in the Reynolds averaged equation for the mean concentration.

the computational effort involved in two phase modeling in flows that are self-similar by adopting a constant diffusivity once the particle turbulent Stokes number is sufficiently less than one.

6. Conclusions

A particle tracking method was shown to be capable of yielding Lagrangian measurements of the dispersion of single droplets in a round jet. Measurements of particle statistics were obtained for a range of characteristic particle response times, nozzle diameters and jet exit velocities. Dispersion as a function of time of flight was quadratic for short times-of-flight; the function became linear for longer times. It was argued that when the local particle Stokes number was less than unity, the particle would behave like a fluid particle. The linear behavior was an indication of the plausibility of the assumption of Batchelor and of Monin and Yaglom that the Lagrangian statistics in a free shear flow are self-preserving in the same manner as the Eulerian statistics. The Lagrangian Peclet numbers of the particles approached the estimated value of the Eulerian Peclet number for a scalar in a round jet. A trend with nozzle size was apparent in the measured Peclet numbers that suggested that unsteadiness around the droplets may have had a small impact on their drag and diffusivity. The results suggest that the calculation of particle dispersion is self-preserving flows such as jets could be simplified considerably once the local particle Stokes number is less than one and the mean velocities of both phases have equilibrated. In such cases, the rate of dispersion of particles could be calculated simply from the eddy diffusivity of the carrier fluid.

Nomenclature

d	droplet diameter (m)
D	nozzle diameter (m)
k	turbulent kinetic energy ($m^2\ s^{-2}$)
L_u	spacing of laser sheets for velocity measurements (m)
Pe	Peclet number
Pr	Prandtl number
R	velocity autocorrelation function
Re	Reynolds number
S_m	acceleration Stokes number
St	Stokes number
t	time (s)
t_u	time-of-flight between laser sheets for velocity measurement (s)
u	axial velocity ($m\ s^{-1}$)
u_T	terminal velocity of droplet ($m\ s^{-1}$)
U	exit velocity of jet ($m\ s^{-1}$)
v	radial velocity ($m\ s^{-1}$)
x_1	axial distance from nozzle (m)
x_2	radial distance from centerline (m)
ε	dissipation rate of turbulent kinetic energy (Eq. (8) only) ($m^2\ s^{-3}$)
ε	eddy diffusivity ($m^2\ s^{-1}$)
η	characteristic length scale (m)
θ	time lag (s)
μ	dynamic viscosity ($kg\ m^{-1}\ s^{-1}$)
ν	kinematic viscosity ($m^2\ s^{-1}$)
ρ	density ($kg\ m^{-3}$)
σ^2	mean square displacement from centerline (dispersion) (m^2)
τ	characteristic time scale (s)

Superscripts

E	Eulerian
L	Langrangian

Subscripts

a	air
d	droplet
e	eddy
g	gas phase
j	based on jet nozzle diameter
k	Kolmogorov
m	momentum
T	temperature

Acknowledgements

This research was supported by the US Air Force Office of Scientific Research under Grant Number AFOSR-F49620-95-1-0276.

References

[1] G.I. Taylor, Diffusion by continuous movements, Proc. London Math. Soc. 20 (1921) 196.
[2] L.P. Wang, D.E. Stock, Dispersion of heavy particles by turbulent motion, J. Atmospheric Sci. 50 (1993) 1897.
[3] S.E. Elghobashi, G.C. Truesdell, Direct simulation of particle dispersion in decaying isotropic turbulence, J. Fluid Mech. 242 (1992) 655.
[4] T. Gotoh, R.S. Rogallo, J.R. Herring, R.H. Kraichnan, Lagrangian velocity correlations in homogeneous isotropic turbulence, Phys. Fluids A 5 (1993) 2846.
[5] Y. Kaneda, Lagrangian and Eulerian time correlations in turbulence, Phys. Fluids A 5 (1993) 2835.
[6] K.D. Squires, J.K. Eaton, Lagrangian and Eulerian statistics obtained from direct numerical simulations of homogeneous turbulence, Phys. Fluids A 3 (1991) 130.
[7] F. Yeh, U. Lei, On the motion of small particles in a homogeneous isotropic turbulent flow, Phys. Fluids A 3 (1991) 2571.
[8] G.K. Batchelor, Diffusion in free turbulent shear flows, J. Fluid Mech. 3 (1957) 67.
[9] A.S. Monin, A.M. Yaglom, Statistical Fluid Mechanics: Mechanics of Turbulence, MIT Press, Cambridge, MA, 1979.
[10] W.H. Snyder, J.L. Lumley, Some measurements of particle velocity auto correlation functions in a turbulent flow, J. Fluid Mech. 48 (1971) 41.

[11] Y. Sato, K. Yamamoto, Lagrangian measurement of fluid-particle motion in an isotropic turbulent field, J. Fluid Mech. 175 (1987) 183.
[12] A.H. Govan, G.F. Hewitt, C.F. Ngan, Particle motion in a turbulent pipe flow, Internat. J. Multiphase Flow 15 (1989) 471.
[13] H. Nicolai, B. Herzhaft, E.J. Hinch, L. Oger, E. Guazzelli, Particle velocity fluctuations and hydrodynamic self-diffusion of sedimenting non-Brownian spheres, Phys. Fluids 7 (1995) 12–23.
[14] Y. Hardalupas, A.M.K.P. Taylor, J.H. Whitelaw, Velocity and particle-flux characteristics of turbulent particle-laden jets, Proc. Roy. Soc. London A 426 (1989) 31.
[15] H. Kobayashi, S.M. Masutani, S. Azuhata, N. Arashi, Y. Hishinuma, Dispersed phase transport in a plane mixing layer, in: Second International Symposium on Transport Phenomena in Turbulent Flows, 1987.
[16] N. Kamalu, F. Wen, T.R. Troutt, C.T. Crowe, J.N. Chung, Particle dispersion by ordered motion in turbulent mixing layers, ASME Forum on Cavitiation and Multiphase Flow, 1988.
[17] N. Kamalu, F. Wen, T.R. Troutt, C.T. Crowe, J.N. Chung, Particle dispersion in developing shear layers, in: International Conference on Mechanics of Two-phase Flows, 1989.
[18] B.J. Lázaro, J.C. Lasheras, Particle dispersion in a turbulent, plane, free, shear layer, Phys. Fluids A 1 (1989) 1035.
[19] G. Hetsroni, M. Sokolov, Distribution of mass, velocity and intensity of turbulence in a two-phase turbulent jet, Trans. ASME Ser. E J. Appl. Mech. (1971) 315.
[20] G.P. Romano, Investigation of particle trajectories and Lagrangian statistics at the outlet of a circular jet, Exp. Thermal Fluid Sci., to appear.
[21] C.J. Call, I.M. Kennedy, Measurements and simulations of particle dispersion in a turbulent flow, Internat. J. Multiphase Flow 18 (1992) 391.
[22] C.J. Call, I.M. Kennedy, Measurements of droplet dispersion in heated and unheated turbulent jets, AIAA J. 32 (1994) 874.
[23] M.R. Wells, D.E. Stock, The effects of crossing trajectories on the dispersion of particles in a turbulent flow, J. Fluid Mech. 136 (1983) 31.
[24] J.S. Shuen, L.D. Chen, G.M. Faeth, Evaluation of a stochastic model of particle dispersion in a turbulent round jet, AIChE J. 29 (1983) 167.
[25] R.W. Dibble, W. Kollmann, R.W. Shefer, Measurements and predictions of scalar dissipation in turbulent flames, in: The 20th International Symposium on Combustion, The Combustion Institute, 1984.
[26] R.A. Antonia, B.R. Satyaprakash, A.K.M.F. Hussain, Measurements of dissipation rate and some other characteristics of turbulent plane and circular jets, Phys. Fluids 23 (1980) 695.
[27] M.R. Maxey, J.J. Riley, Equation of motion for a small rigid sphere in nonuniform flow, Phys. Fluids 26 (1983) 883.
[28] G.M. Faeth, Evaporation and combustion of sprays, Progr. Ener. Combustion Sci. 9 (1983) 1.
[29] P.G. Saffman, The lift on a small sphere in a slow shear flow, J. Fluid Mech. 22 (1965) 385.
[30] A.D. Gosman, E. Ionnides, Aspects of computer simulation of liquid-fueled combustors, J. Energy 7 (1983) 482.
[31] B.D. Shaw, Personal Communication (1995).
[32] J.O. Hinze, Turbulence, McGraw-Hill, New York, 1975.
[33] R. Chevray, N.K. Tutu, Intermittency and preferential transport of heat in a round jet, J. Fluid Mech. 88 (1978) 133.
[34] L. Tang, F. Wen, Y. Yang, C.T. Crowe, J.N. Chung, T.R. Troutt, Self-organizing particle dispersion mechanism in a plane wake, Phys. Fluids A 4 (1992) 2244.
[35] F. Odar, W.S. Hamilton, Forces on a sphere accelerating in a viscous fluid, J. Fluid Mech. 18 (1964) 302.
[36] S.K. Karanfilian, T.J. Kotas, Drag on a sphere in unsteady motion in a liquid at rest, J. Fluid Mech. 87 (1978) 85.